


Two-Dimensional Plasmonic Grating for Intraocular Pressure Sensing

Yong Ho Kwon¹, Jayar Fernandes^{1*}, Jae-Jun Kim¹, Mary Ann Croft^{3,4}, Hwei Liu¹, Paul L. Kaufman^{3,4}, and Hongrui Jiang^{1,2,3,4**} 

¹Department of Electrical and Computer Engineering, University of Wisconsin-Madison, Madison, WI 53705 USA

²Department of Materials Science and Engineering, University of Wisconsin-Madison, Madison, WI 53705 USA

³Department of Ophthalmology and Visual Sciences, University of Wisconsin-Madison, Madison, WI 53705 USA

⁴The McPherson Eye Research Institute, University of Wisconsin-Madison, Madison, WI 53705 USA

* Student Member, IEEE

** Fellow, IEEE

Manuscript received August 8, 2019; revised September 1, 2019; accepted September 14, 2019. Date of publication September 18, 2019; date of current version October 4, 2019.

Abstract—Glaucoma is a group of characteristic optic neuropathies that collectively are the leading cause of irreversible blindness globally. Elevated intraocular pressure (IOP) is the major causal risk factor. While the fundamental mechanisms of the IOP elevation and consequent optic neuropathy are not well understood, recent studies have indicated that there may be pressure spikes directed at the optic nerve head during accommodation and that IOP may not be homogeneous throughout the eye. To facilitate the *in situ* and *in vivo* measurement of IOP in various locations within the vitreous and facilitate measurement of accommodative IOP spikes at the ONH, here, we report the development of an implantable, biocompatible, and miniaturized IOP sensor using 2-D plasmonic grating that generates structural color. The change of the grating period with pressure between 0 and 50 mmHg results in a change in the visible color, allowing us to observe small changes in pressure without additional electronics.

Index Terms—Electromagnetic wave sensors, glaucoma, intraocular pressure (IOP), optical nerve head (ONH), surface plasmon.

I. INTRODUCTION

Glaucoma is a family of chronic, degenerative optic neuropathies that affect millions of people worldwide. It is estimated that 80 million people will have glaucoma in 2020 [1], with approximately 10% being bilaterally blind from irreversible optic nerve damage, making it the world's leading cause of irreversible blindness [2]. Glaucoma is associated causally with intraocular pressure (IOP); i.e., glaucoma risk increases with increasing IOP. Lowering IOP is currently the only therapy for glaucoma [3]. However, the basic disease pathophysiology of glaucoma is still poorly understood, and study of its biological mechanisms is critical for its prevention and cure.

Research in recent years [4], [5] reveals a constellation of evidence demonstrating that the process of accommodation may also play a role in the onset of glaucoma. Specifically, there may be a pressure gradient toward the optic nerve head (ONH) during accommodation, the process by which we focus on objects at close range. Furthermore, these accommodative pressure spikes may increase with age as the function of the accommodative apparatus changes [6]–[9]. Measuring and studying such accommodative IOP spikes may lead to better understanding of the pathophysiology of glaucoma.

Historically, IOP has been measured by applanation tonometry, requiring contact with the cornea (the anterior surface of the eye). The technique assumes a uniform, homogeneous pressure within the whole eye. However, the ONH interfaces with the vitreous compartment at the posterior pole of the eye. The vitreous contains various structural components (Cloquet's Canal, cistern structure) that may act to channel fluid movement toward the region of the ONH during accommodation. This suggests that pressure within the eye may not be homogeneous

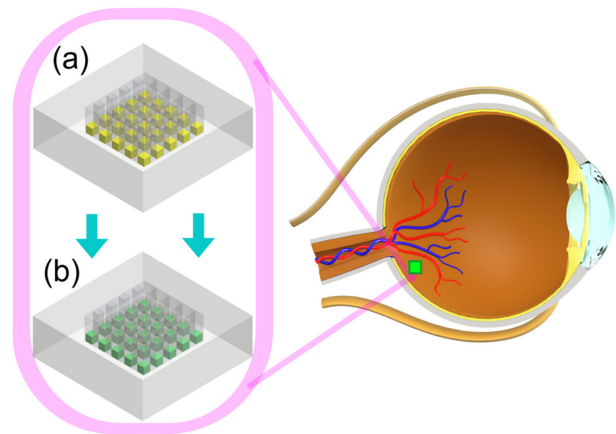


Fig. 1. Illustration of the IOP sensor implanted near the ONH. (a) Sensor in its initial state. (b) Change in color after change in IOP.

but rather is location dependent. In order to monitor accurately in real time the dynamic changes in IOP in various locations within the vitreous, and particularly the accommodative IOP spikes at the ONH, it is desirable to have a sensing modality that allows for the *in situ* and *in vivo* measurement of the IOP. However, the relatively large size and absence of flexibility makes it impossible to attach to the curved surfaces in the eye, and the requirement for additional electronic modules such as power supply and powered data transfer make currently available commercial pressure sensors unfit for this application [10]–[13]. Consequently, as shown in Fig. 1, to directly and continuously measure the pressure near the ONH region, implantable sensors are needed that are miniaturized, biocompatible, low power, and sensitive to the small pressure changes that are expected near the ONH region. In this

Corresponding author: Hongrui Jiang (e-mail: hongrui@engr.wisc.edu).

Associate Editor: X. Shu.

Digital Object Identifier 10.1109/LENS.2019.2942212

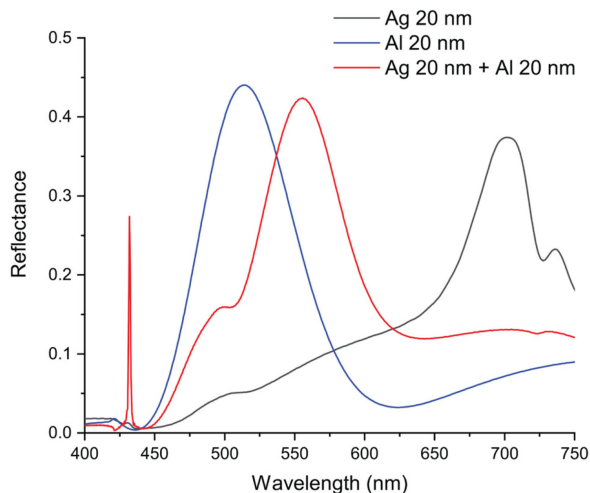


Fig. 2. FDTD simulation results of the grating structure with different materials.

article, we report a flexible, passive (thus zero power consumption), and biocompatible IOP sensor based on the concept of surface plasmon of metal 2-D gratings. Embedding nanophotonic gratings with an elastomeric material allows for the conversion of a small change in IOP to optical data in the form of a quantifiable variation in color. The sensor is a purely optical device that does not require an accompanying energy source and can endure the temperature and the watery environment within the eye. In addition, the sensor does not require electric data transfer modules since it displays visual information that can be directly obtained externally. Furthermore, since the output data from the sensors is a color change, as shown in Fig. 1, we can take advantage of real-time and dynamic measurement techniques through image processing.

II. PRINCIPLE AND STRUCTURE

The overall sensor structure comprises of an array of 2-D gratings embedded in a 50- μm -thick polydimethylsiloxane (PDMS) membrane that was suspended over an air cavity chamber to form a sealed pressure sensor. The structural color in the visible range from surface plasmon resonance of the metallic 2-D gratings provides information about the IOP (0–50 mmHg [14]). A 2-D grating structure was chosen in order to accommodate the radial expansion of the sensor membrane along both in-plane directions in response to a pressure change, allowing for the shift in the grating period along both directions, resulting in variations in color patterns [15]–[21].

Fig. 2 shows the comparison of the reflectance peaks of the grating structures composed of different metals such as aluminum (Al), silver (Ag), and Al layer on top of Ag (Ag + Al). The parameters used in the Finite difference time domain (FDTD) simulation were: Ag thickness – 20 nm; Al thickness – 20 nm; refractive index: PDMS – 1.4, Ag – 0.125, and Al – 0.958 at the 550 nm wavelength. In this work, we selectively removed the metal layers deposited on the top of the flexible polymer substrates to fabricate 2-D grating structures by using the adhesion force between the photoresist (SU-8) and metals. Although Al itself covers a broad range of visible wavelengths, an Al layer deposited on top of the flexible polymer substrate is hard to remove to form the gratings. On the other hand, Ag has a relatively weak adhesion force, making it easier to remove from the surface on which it is deposited. Nevertheless, the covering range of Ag in the visible wavelengths is not as broad as Al. The highest peak of Ag is near 700 nm, which is close to infrared. This would make it difficult to detect visible color

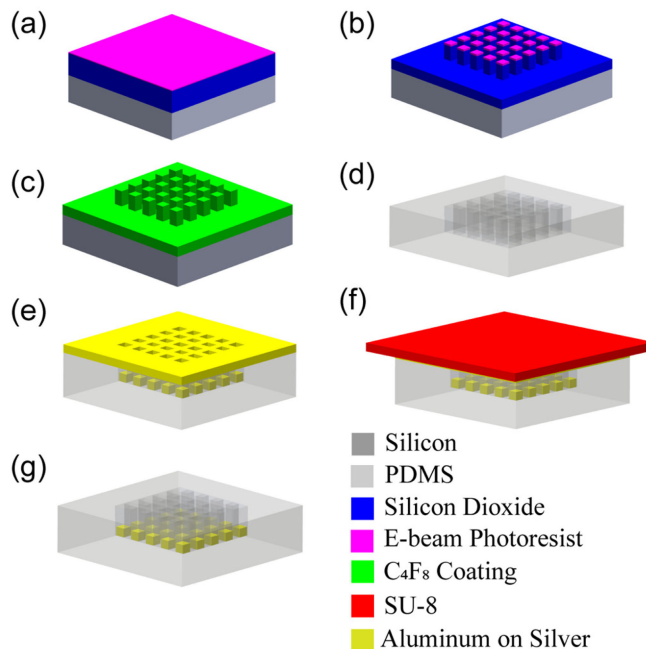


Fig. 3. Illustration of the fabrication process for the IOP sensor. (a) SiO_2 deposition and lithography. (b) Resist development and RIE etching. (c) Teflon coating. (d) PDMS molding. (e) Evaporation of Ag and Al. (f) Alignment of SU-8 for removing the metal surface layer. (g) IOP sensor formed.

changes in the grating. For these reasons, a combined metal layer of Al deposited directly on top of Ag was selected. Ag serves as the anti-adhesion layer between Al and the flexible polymer, which makes the removal of the unnecessary metal easier, and consequently allows wide coverage of the visible wavelengths.

III. FABRICATION

Fig. 3 shows the fabrication process of the pressure sensor that consists of a thin PDMS layer and 2-D metal grating structures. First, 500 nm of silicon dioxide (SiO_2) was deposited onto a clean Si wafer using plasma enhanced chemical vapor deposition. Negative electron-beam resist (ma-N 2401, Micro Resist Technology) was then spin-coated on top of the SiO_2 layer as shown in Fig. 3(a). Nanometer scale 2-D gratings were subsequently defined by electron-beam lithography. The period, width, and gap of the grating structures are 300, 100, and 200 nm, respectively. After defining the patterns, reactive ion etching (RIE) was performed to create SiO_2 gratings with a height of 350 nm [see Fig. 3(b)], which was used to make the PDMS mold. A gas mixture of trifluoromethane (CHF_3) and argon (Ar) were used to anisotropically etch the SiO_2 layer, followed by the removal of the photoresist. An anti-stiction layer was formed for easy demolding [see Fig. 3(c)]. A PDMS mixture was spin coated directly on the template and cured under 150 $^\circ\text{C}$ to create a mold [see Fig. 3(d)]. Additionally, 20 nm of Ag was deposited directly on the PDMS mold and another 20 nm of Al was deposited on top of the Ag layer by e-beam evaporator [see Fig. 3(e)]. Finally, unnecessary surface materials on PDMS were selectively removed by using cured SU-8 on quartz glass [see Fig. 3(f)]. The 2-D gratings are, thus, left behind to function as the IOP sensor [see Fig. 3(g)].

IV. EXPERIMENTAL SETUP

We aim to develop a passive IOP sensor that can be implanted near the ONH region. For the effective characterization of the sensor,

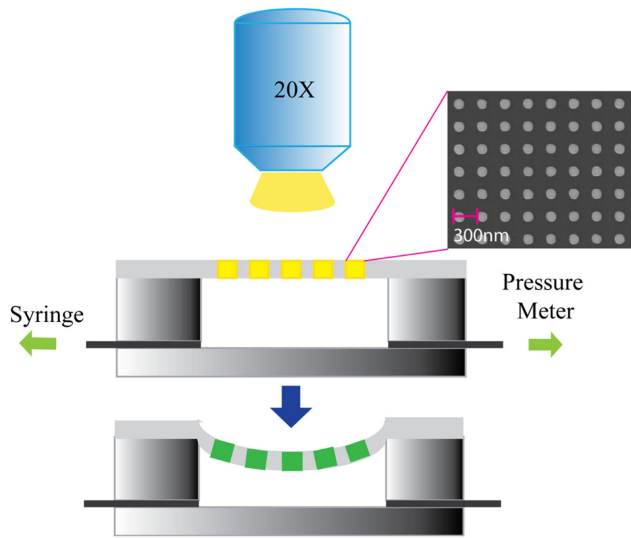


Fig. 4. Schematic of the experimental setup for pressure sensor characterization.

we mimicked a fundus photography setup and centrally aligned and bonded the pressure sensor to a cavity 1 mm in height and 5 mm in diameter, molded into a PDMS chamber. The cavity inside the chamber was filled with air, and a channel on each side was connected to a syringe (15 mL/min) and a pressure gauge (Honeywell HSC-DANN001PGAA5) to adjust and record the pressure change inside the chamber. The overall setup for sensor characterization is shown in Fig. 4. A microscope lamp (LV-HL50 W Nikon Halogen Bulb) was used to illuminate the sensor under normal incidence and a 20 \times objective lens was used to collect the reflected light from the sensor. Applying a negative pressure inside the chamber utilizing the syringe resulted in a deformation of the sensor membrane, which increased the curvature, increasing the period in both in-plane directions and decreasing the duty cycle of the 2-D metal (Ag + Al) gratings. The changed period and duty cycle resulted in a blue shift of the reflected color to shorter wavelengths from yellow to green as shown in Fig. 5. In order to detect and quantify the change in the reflected color with minimal hardware usage, we opted for an approach through RGB image analysis of the segmented images of the sensor captured through the microscope.

V. RESULTS

Fig. 5 shows the images of a fabricated IOP sensor under the experimental setup and the corresponding RGB data analysis that was conducted on the optical images, after segmenting the grating using a k-means clustering algorithm. There are 40 000 2-D gratings stored inside a single square.

From this design, under the experimental setup, we could detect the color change of the IOP sensor via the change in the applied pressure, which was matched with the RGB analysis [22]. We observed an increase in the peak green and peak blue values, with a larger increase in the blue component, and a decrease in the peak red component, as the pressure increased, showing a blue shift in the reflected spectrum.

This value was, then, plotted against the pressure, along with the peak R, G, B values. The R component showed a 5.3% decrease and the peak blue component showed a 17% increase from their initial values, as the pressure was increased along the different stages.

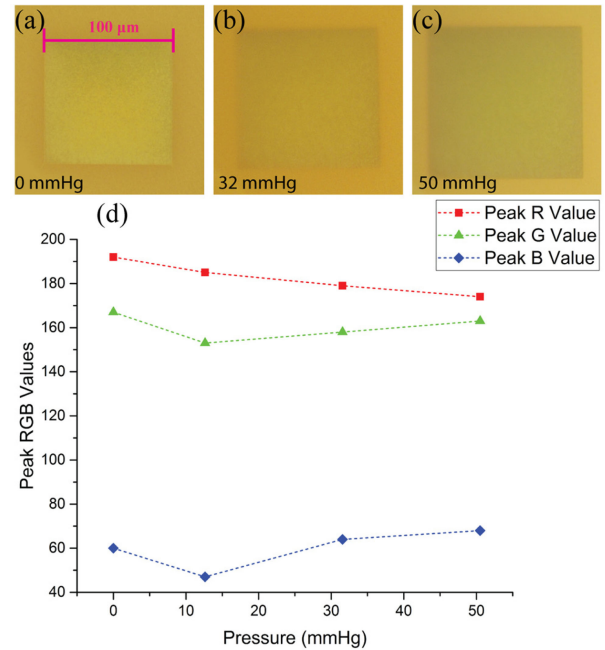


Fig. 5. Optical images of the pressure sensor (a) in the initial state and (b), (c) after the applied pressure increased. (d) RGB analysis of the segmented images from above, indicating the trends in the R, G, and B values as the applied pressure increased.

VI. CONCLUSION

This article reports a unique biocompatible and flexible optical sensor based on near wavelength 2-D gratings that can correlate minor change in pressure to changes in observed color of reflected light. The FDTD simulations, along with optical measurements, validated the possibility of passive measurement in the IOP range. Future works include integrating micro needles on the back of the sensor and developing surgical procedures to fix (remove) the sensor onto (from) the retina, calibration and optimizing the sensitivity of the sensor, and simulating the reflectance spectrum with spectrometer measurement. Optimized calibration routines with real-time image processing algorithms will be developed to achieve highly accurate correlation between IOP and visible color. The ultimate goal is to implant the sensor on the retina of the eye of a primate model near the ONH to study the pathophysiology of the glaucoma.

ACKNOWLEDGMENT

This work was supported by NSF under Grant DMR-1625348 for the EBL. This project utilized shared fabrication facilities in Wisconsin Centers for Nanoscale Technology, University of Wisconsin-Madison, Madison, WI, USA. This work was supported by the Research to Prevent Blindness 2016 Stein Innovation Award to H. Jiang. (Yong Ho Kwon, Jayer Fernandes, and Jae-Jun Kim contributed equally to this work.)

REFERENCES

- [1] H. A. Quigley and A.T. Broman, "The total number of people with glaucoma worldwide in 2010 and 2020," *Br. J. Ophthalmol.*, vol. 910, pp. 262-267, 2006.
- [2] R. N. Weinreb, T. Aung, and F. A. Medeiros, "The pathophysiology and treatment of glaucoma: A review," *JAMA*, vol. 311, pp. 1901-1911, 2014.
- [3] A. Heijl, "Glaucoma treatment: By the highest level of evidence," *Lancet*, vol. 385, pp. 1264-1266, 2015.
- [4] M. A. Croft, E. Lütjen-Drecoll, and P. L. Kaufman, "Age-related posterior ciliary muscle restriction - A link between trabecular meshwork and optic nerve head pathophysiology," *Exp. Eye Res.*, vol. 158, pp. 187-189, 2017.

- [5] P. L. Kaufman, E. Lütjen-Drecoll, and M. A. Croft, "Presbyopia and Glaucoma: Two diseases, one pathophysiology? The Friedenwald lecture," *Invest Ophthalmol. Vis. Sci.*, vol. 60, no. 5, pp. 1801–1812, 2019.
- [6] M. Croft, A. Glasser, G. Heatley, J. P. McDonald, T. Ebbert, and P. L. Kaufman, "Accommodative ciliary body and lens function in rhesus monkeys. I: Normal lens, zonule and ciliary process configuration in the iridectomized eye," *Invest Ophthalmol. Vis. Sci.*, vol. 47, pp. 1076–1086, 2006.
- [7] M. Croft, J. P. McDonald, N. V. Nadkarni, T. L. Lin, and P. L. Kaufman, "Age-related changes in centripetal ciliary body movement relative to centripetal lens movement in monkeys," *Exp. Eye Res.*, vol. 89, pp. 824–832, 2009.
- [8] M. A. Croft, J. P. McDonald, A. Katz, T. L. Lin, E. L. Drecoll, and P. L. Kaufman, "Extralenticular and lenticular aspects of accommodation and presbyopia in human versus monkey eyes," *Invest Ophthalmol. Vis. Sci.*, vol. 54, pp. 5035–5048, 2013.
- [9] E. A. Balazs and J. L. Denlinger, "Aging changes in the vitreous," in *Aging and the Human Visual Function*. Modern Aging Research Series, vol. 2, New York: Liss, 1982, pp. 45–57.
- [10] S. Gong *et al.*, "A wearable and highly sensitive pressure sensor with ultrathin gold nanowires," *Nat. Commun.*, vol. 5, 2014, Art. no. 3132.
- [11] S. C. B. Mannsfeld *et al.*, "Highly sensitive flexible pressure sensors with microstructured rubber dielectric layers," *Nat. Mater.*, vol. 9, pp. 859–864, 2010.
- [12] J. Wang *et al.*, "A highly sensitive and flexible pressure sensor with electrodes and elastomeric interlayer containing silver nanowires," *Nanoscale*, vol. 7, pp. 2926–2932, 2015.
- [13] Y. Joo *et al.*, "Silver nanowire-embedded PDMS with a multiscale structure for a highly sensitive and robust flexible pressure sensor," *Nanoscale*, vol. 7, pp. 6208–6215, 2015.
- [14] E. J. Lee, T. W. Kim, R. N. Weinreb, and H. Kim, "Reversal of lamina cribrosa displacement after intraocular pressure reduction in open-angle glaucoma," *Ophthalmol.*, vol. 120, no. 3, pp. 553–559, 2013.
- [15] W. L. Barnes, A. Dereux, and T. W. Ebbesen, "Surface plasmon subwavelength optics," *Nature*, vol. 424, pp. 842–830, 2003.
- [16] P. Mulvaney, "Surface plasmon spectroscopy of nanosized metal particles," *Langmuir*, vol. 12, no. 3, pp. 788–800, 1996.
- [17] R. H. Ritchie, E. T. Arakawa, J. J. Cowan, and R. N. Hamm, "Surface-plasmon resonance effect in grating diffraction," *Phys. Rev. Lett.*, vol. 21, 1968, Art. no. 1530.
- [18] B. Lamprecht *et al.*, "Metal nanoparticle gratings: influence of dipolar particle interaction on plasmon resonance," *Phys. Rev. Lett.*, vol. 84, 2000, Art. no. 4721.
- [19] Z. Han, E. Forsberg, and S. He, "Surface plasmon Bragg gratings formed in metal-insulator-metal waveguides," *IEEE Photon. Technol. Lett.*, vol. 19, no. 2, pp. 91–93, Jan. 2007.
- [20] M. Kang, J. J. Kim, Y. J. Oh, S. G. Park, and K. H. Jeong, "A deformable nanoplasmonic membrane reveals universal correlations between plasmon resonance and surface enhanced raman scattering," *Adv. Mater.*, vol. 26, pp. 4510–4514, 2014.
- [21] Y. Shen, V. Rinnerbauer, I. Wang, V. Stelmakh, J. D. Joannopoulos, and M. Soljacic, "Structural colors from fano resonance," *ACS Photon.*, vol. 2, no. 1, pp. 27–32, 2015.
- [22] J. Fernandes, Y. H. Kwon, J. Kim, H. Liu, and H. Jiang, "High contrast grating based strain sensor for intraocular applications," *J. Microelectromech. Syst.*, vol. 27, no. 4, pp. 599–601, 2018.